THE JOURNAL OF PHYSICAL CHEMISTRY B

Article

pubs.acs.org/JPCB

Theoretical and Experimental Studies on Vibrational Energy Relaxation of the CO Stretching Mode of Acetone in Alcohol Solutions

Masahiro Higashi,[†] Satori Hirai,[‡] Motohiro Banno,[§] Kaoru Ohta,[§] Shinji Saito,*[,†] and Keisuke Tominaga*[,‡,§]

[†]Institute for Molecular Science, Myodaiji, Okazaki, 444-8585, Japan

[‡]Graduate School of Science, Kobe University, Nada, Kobe 657-8501 Japan

[§]Molecular Photoscience Research Center, Kobe University, Nada, Kobe 657-8501 Japan

Supporting Information

ABSTRACT: The vibrational energy relaxations (VERs) of the CO stretching mode of acetone and its complexes with alcohols are investigated by sub-picosecond pump−probe spectroscopy and molecular dynamics simulation. The time constants of the vibrational energy relaxation of the free acetone and that of the 1:1 complex are 4.4 and 2.3 ps for methanol solvent and 5.2 and 1.8 ps for 1-proponal solvent, respectively. The VER rate is accelerated a few times by formation of the hydrogen bond. This acceleration of the vibrational energy relaxation is successfully reproduced by the Landau−Teller method calculated from the molecular dynamics simulation. Molecular dynamics simulations reveal that the VER time of acetone with the hydrogen bond is largely affected by the solute polarization induced by solvent molecules.

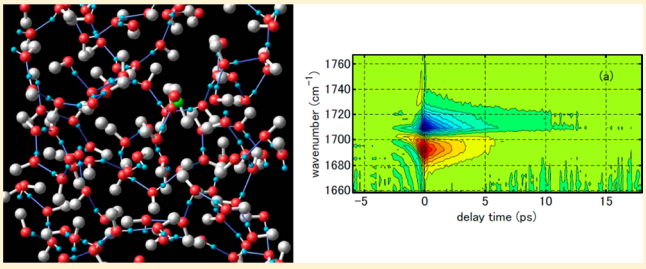

INTRODUCTION

Hydrogen bonds play an important role in determining the stability of three-dimensional structures of many chemical complexes and biological macromolecules.[1−3] In these hydrogen-bonded complexes, various dynamical processes such as reactivity and energy relaxation are strongly influenced by intramolecular hydrogen bonds as well as intermolecular ones. Solute molecules in protic solvents such as water and alcohol often make hydrogen bonds with solvent molecules, and static and dynamic properties of hydrogen bonds influence reactivity in such solvents. Since the vibrational modes in liquids are sensitive probes for surrounding the microscopic environment, effects of hydrogen bonds on vibrational dynamics have been investigated by time-resolved infrared (IR) spectroscopy extensively.[4−12] The vibrational energy relaxation (VER) is one of the important vibrational dynamics, which has been studied for hydrogen-bonded complexes in nonpolar solvents and solute molecules in hydrogen-bonding solvents. It has been shown that the VER is significantly affected by the formation of a hydrogen bond.

In the previous work, we investigated vibrational energy relaxation of 9-fluorenone (FL) in 1-octanol by sub-picosecond pump−probe spectroscopy.[13] The IR absorption spectrum of FL in alcohol shows three distinct contributions from the free FL, its complex with one alcohol molecule, and that with two molecules. The time constant of the vibrational energy relaxation (VER) of the free FL is 4.7 ± 0.1 ps, and that of the 1:1 complex is 2.3 ± 0.1 ps. We interpreted the acceleration of the VER due to hydrogen bond formation in terms of the Fermi golden rule. The transition rate is determined by the vibrational density of states (VDOS), coupling strength, and energy gap. The formation of a hydrogen bond could influence all of these factors. Unlike the VER of the OH stretching mode of water, the energy shift due to the bond formation of the CO stretching vibration is about 10 cm^{-1}, and it is not likely that the energy gap change has a major effect on the VER time. Instead, an increase in the VDOS may be the cause for this acceleration of the relaxation. Quantum chemical calculations show that there are several intermolecular vibrational modes with frequencies less than 100 cm^{-1} for the FL:methanol complex, which may be accepting modes in the relaxation process. It is likely that the effective dissipation of energy from the CO stretching mode in the hydrogen-bonded complexes results from the increase in the VDOS through a combination of intramolecular fingerprint and intermolecular low-frequency modes.

In liquid state, solvent molecules surrounding the hydrogen-bonded complexes continuously fluctuate and exert time-dependent interactions to the complexes. Therefore, it may be more appropriate to include such fluctuation to evaluate the

Special Issue: Paul F. Barbara Memorial Issue

Received: October 26, 2012
Revised: December 24, 2012
Published: January 10, 2013

Table 1. Charges (in au) and Dipoles (in D) of Acetone Calculated from MD Simulations with the CRK Method[a]

solvent	N_{HB}	Q_O	$Q_{C(O)}$	$Q_{C(H)}$	Q_H	dipole
gas		−0.502	0.724	−0.560	0.150	2.94
methanol	total	−0.597 (0.038)	0.774 (0.055)	−0.571 (0.035)	0.161 (0.026)	4.07 (0.39)
	0	−0.543 (0.017)	0.728 (0.039)	−0.556 (0.030)	0.155 (0.023)	3.62 (0.27)
	1	−0.595 (0.025)	0.776 (0.050)	−0.572 (0.034)	0.161 (0.026)	4.04 (0.29)
	2	−0.633 (0.031)	0.798 (0.056)	−0.577 (0.037)	0.165 (0.029)	4.41 (0.33)
1-propanol	total	−0.579 (0.035)	0.764 (0.049)	−0.570 (0.032)	0.159 (0.025)	3.88 (0.37)
	0	−0.531 (0.015)	0.724 (0.034)	−0.558 (0.026)	0.154 (0.021)	3.47 (0.26)
	1	−0.582 (0.024)	0.769 (0.046)	−0.572 (0.031)	0.160 (0.025)	3.90 (0.28)
	2	−0.615 (0.030)	0.785 (0.053)	−0.574 (0.035)	0.163 (0.027)	4.24 (0.32)

[a]Standard deviations are in parentheses.

VER rate. The Landau−Teller expression is a formalism based on the time-correlation function of the force exerted on the state, which can be derived from the Fermi golden rule. The transition rate between two vibrational levels i and f with energies E_i and E_f can be expressed as

$$k_{f\leftarrow i} = \frac{1}{\hbar^2}|q_{i,f}|^2 \int_{-\infty}^{\infty} dt e^{i\omega_{i,f}t}\langle \hat{F}(t)\hat{F}(0)\rangle \quad (1)$$

where $\omega_{i,f} = (E_i - E_f)/\hbar$, $q_{i,f}$ is the matrix element of the coordinate operator of the oscillator between the i- and f-states, and $\hat{F}(t)$ is the operator of the total force exerted on the vibrational mode by the solvent.[14] This expression allows us to investigate the solvent fluctuation effect on the VER rate of the hydrogen-bonded complex.

Effects of hydrogen bonds on VER have been theoretically studied by several groups.[15−26] Bruehl and Hynes carried out a molecular dynamics (MD) simulation to estimate VER for a model hydrogen-bonded complex in a model polar aprotic solvent.[15] They found that interactions of the solute with first solvent shell molecules provide the dominant source of the relaxation forces. Morita and Kato studied VER of the antisymmetric stretching mode of azide ion in water by MD simulation.[17] They found that the solute electronic polarization plays an important role in its fast relaxation. They also pointed out that the intramolecular vibrational redistribution is induced by the solute internal anharmonicity and solute−solvent coupling.

In this study, we have investigated the hydrogen bond effect on the VER by sub-picosecond IR pump−probe spectroscopy and MD simulation. The system we chose is the CO stretching mode of acetone in alcohol solvents. Experimentally, we obtained the VER times of the CO stretching mode of non-hydrogen-bonded and hydrogen-bonded acetone in methanol and 1-propanol. From classical MD simulation, we show that the acceleration of the VER results from the hydrogen bond between the solute and solvent in alcohol solutions.

EXPERIMENTAL SECTION

Details of the IR pump−probe apparatus were described elsewhere.[11] Briefly, a home-built optical parametric amplifier and difference frequency generator, which are pumped by a Ti:sapphire regenerative amplifier, delivered short pulses in the IR region with a pulse width of about 150 fs. The output pulse was divided into three components: pump, probe, and reference pulses. The probe and reference pulses were detected independently by two 32-channel mercury cadmium telluride (MCT) array detectors after passing through a monochromator. The sample was contained in a cell with an optical path length of 0.1 mm and CaF_2 windows. Acetone, methanol, and 1-propanol were purchased from Sigma-Aldrich and used without further purification. The measurements were performed at room temperature (20 °C).

COMPUTATIONAL DETAILS

We have performed two MD simulations; one is acetone in methanol, and the other is acetone in 1-propanol. The methanol solution system consists of 1 acetone and 215 methanol molecules, while the 1-propanol solution system consists of 1 acetone and 124 1-propanol molecules. In these systems, a cubic box with periodic boundary conditions was used, and the box lengths are 24.6 and 25.0 Å for the methanol and 1-propanol solutions, respectively. The OPLS-AA force field was used for methanol and 1-propanol.[27,28] The van der Waals (vdW) interactions between acetone and alcohols were also treated by the OPLS-AA force field. (For acetone, see below.) For the long-range electrostatic interaction, we used the tapering method implemented in the TINKER program,[29] where the electrostatic interaction is smoothly truncated at 12 Å. A cutoff length of 12 Å was also used for the vdW interactions. The equations of motion were integrated using the leapfrog algorithm with a time step of 1 fs. The temperature was 300 K. MD simulations were performed for 20 ns for both systems. During the MD simulations, the solute geometry was fixed at the gas-phase optimized geometry by using the SHAKE method. The CH and OH bonds in the solvent molecules were also fixed by using the SHAKE method. All the MD simulations were carried out using the AMBERPLUS program package.[29−31]

In this study, we have examined the effect of polarization of solute by solvent molecules on the vibrational relaxation. The polarization was considered with the charge response kernel (CRK) method.[32] In the CRK model, the solute charges $\{Q_a; a = 1, 2, ..., N_{solute}\}$, where N_{solute} is the number of atoms in a solute molecule and $N_{solute} = 10$ for acetone, are fluctuated by the external electrostatic potential on the solute atoms $\{\Phi_a\}$

$$Q_a = Q_a^0 + \sum_b K_{ab}\Phi_b \quad (2)$$

where Q_a^0 and K_{ab} are the gas-phase charge and CRK, respectively, which were calculated by the M06-2X/6-311G-(2d,2p) density functional method at the gas-phase optimized geometry.[33] The electrostatic potential (ESP) charge fitting was used to obtain Q_a^0. The CRK, K_{ab}, was evaluated by using the numerical differentiation of Q_a^0 with respect to Φ_b. For the hydrogen atoms of the methyl groups, Q_a^0 and K_{ab} were symmetrized by averaging those obtained by the electronic structure calculation. All of the electronic structure calculations

dx.doi.org/10.1021/jp310621p | J. Phys. Chem. B 2013, 117, 4723−4731

were performed using the GAMESS quantum package,[34] where we implemented our routines.

Tables 1 and S1 (Supporting Information) summarize Q_a^0 and K_{ab} used in the MD simulations. It is noted that the calculated dipole moment from $\{Q_a^0\}$, 2.94 D, is in good agreement with the experimental result in the gas phase, 2.93 D.[35] The dipole moment in solution is enhanced by the solvent; the averages of dipole moment are 4.07 and 3.88 D in methanol and 1-propanol, respectively (Table 1). To examine the effect of the fluctuating charges, we carried out MD simulations with fixed charges. The fixed charges are defined as the averaged charges calculated from the MD simulations with the CRK method (Table 1).

EXPERIMENTAL RESULTS AND ANALYSIS

Figure 1a shows the IR absorption spectrum of acetone in methanol. The CO stretching mode of acetone shows a band

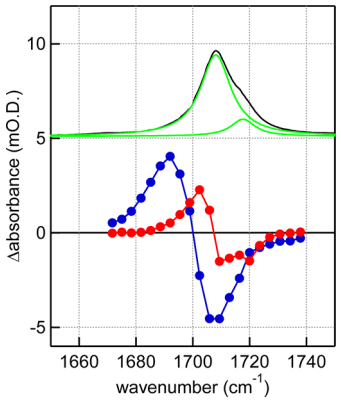

Figure 1. (upper) Static IR absorption spectrum of acetone in methanol (black), which is decomposed into two Lorentzian functions (green). (lower) Decay-associated spectra of the 4.4 ps component (red) and 2.3 ps component (blue) obtained by the global fitting.

with a peak at 1709 cm^{-1} with a shoulder at around 1700 cm^{-1}. In the case of FL in alcohol solvents, pronounced structures with two peaks and a shoulder are observed in the CO stretching band.[13] We concluded that these structures are due to the non-hydrogen-bonded (free) FL, 1:1 complex (FL:alcohol), and 1:2 complex (FL:$(alcohol)_2$) from comparison with calculation by density functional theory for these molecular species. The peak wavenumbers are 1721, 1713, and 1700 cm^{-1} for free FL, 1:1 complex, and 1:2 complex, respectively. From the analogy of the previous study on FL in alcohol, we simulate the CO stretching band of acetone with a sum of two Lorentzian functions, and the high- and low-frequency components are assigned to free acetone and the 1:1 complex with methanol, respectively. The peak frequencies are 1719 and 1709 cm^{-1} for the acetone/methanol system. In 1-propanol, a similar band shape is observed for the CO stretching mode (data are not shown).

The frequency-resolved pump−probe signals of acetone in methanol are shown in Figure 2a. The blue region corresponds to the ground state bleach and the stimulated emission, and the red region, to the transient absorption. In Figure 2b, we show plots of the transient decay of the $v = 0 \rightarrow v = 1$ bleach/stimulated emission and $v = 1 \rightarrow v = 2$ excited state absorption of the C═O stretching mode. Figure 3 displays the time-resolved difference spectra obtained from Figure 2 at a delay time of 0.75, 1.5, and 3.0 ps. A global fitting analysis with a

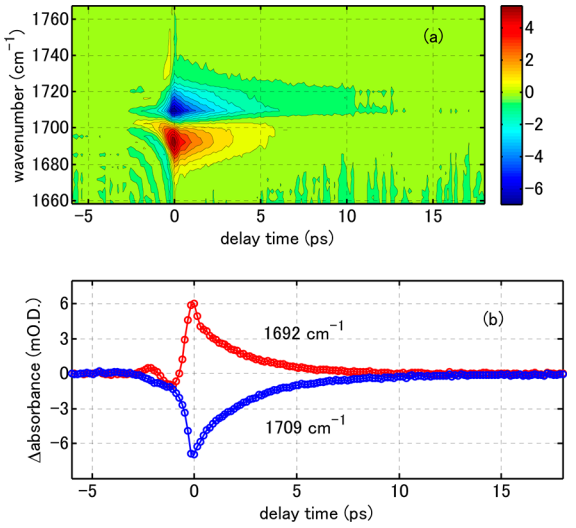

Figure 2. (a) Frequency-resolved pump−probe signals of acetone in methanol. (b) Plots of the transient decay of the $v = 0 \rightarrow v = 1$ bleach/stimulated emission (blue) and $v = 1 \rightarrow v = 2$ excited state absorption (red) of the C═O stretching mode.

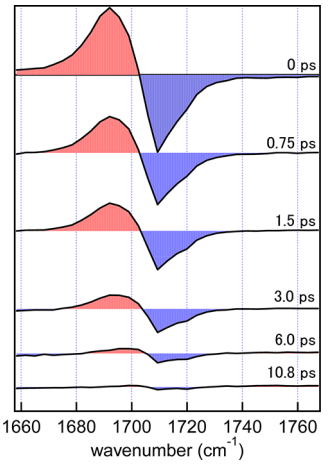

Figure 3. Time-resolved difference spectra obtained from Figure 2 of acetone in methanol. The delay time is shown in the figure.

biexponential function was performed in the time range after 0.45 ps to avoid coherent artifact. The decay time constants obtained by the fitting are 4.4 and 2.3 ps for the high- and low-frequency components. The two decay-associated spectra are shown in Figure 1b. The peak wavenumbers of the bleach components of the decay-associated spectra correspond to the Lorentzian components in the steady-state spectrum. Therefore, we assign that the decay time constants of 4.4 and 2.3 ps are the VER times of free acetone and the 1:1 complex, respectively. Similarly, for the system of acetone in 1-propanol, we obtained VER times of 5.2 and 1.8 ps for free acetone and the 1:1 complex, respectively. The transient data are shown in Figure 4. Therefore, we conclude that the VER rate is accelerated a few times by the hydrogen bond formation.

MOLECULAR DYNAMICS SIMULATION; RESULTS AND DISCUSSION

We here show the VER of the CO stretching mode of acetone in alcohols calculated from the MD simulations. We analyzed two systems; one is acetone in methanol, and the other is

dx.doi.org/10.1021/jp310621p | J. Phys. Chem. B 2013, 117, 4723−4731

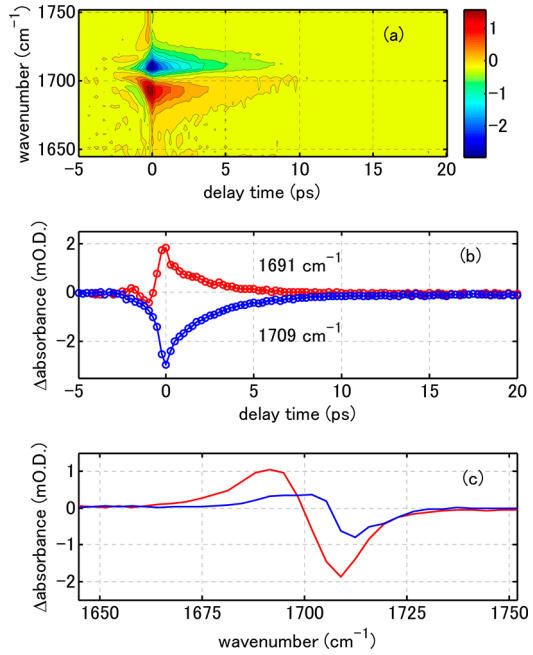

Figure 4. (a) Frequency-resolved pump−probe signals of acetone in 1-propanol (upper). (b) Plots of the transient decay of the $v = 0 \rightarrow v = 1$ bleach/stimulated emission (blue) and $v = 1 \rightarrow v = 2$ excited state absorption (red) of the C═O stretching mode. (c) Decay-associated spectra of the 5.2 ps component (blue) and 1.8 ps component (red) obtained by global fitting.

acetone in 1-propanol. In addition, to examine the effect of solute polarization, we adopted the polarizable and fixed charge models for acetone. Thus, we performed four different MD simulations in total.

Figure 5 shows radial distribution functions for the distance between the oxygen atom of acetone and the hydrogen atom of the hydroxyl group of alcohol, r_{O-H_O}. There is no significant difference between the polarizable and fixed charge models. In both charge models, there is a sharp peak at around 1.8 Å. This peak corresponds to the hydrogen bond between acetone and alcohol molecules in the first solvation shell. The peak intensity in 1-propanol is stronger than that in methanol. This is due to the fact that the number density of 1-propanol is smaller than that in methanol. The first minimum is found at 2.80 and 2.90 Å for methanol and 1-propanol in both charge models. From this result, we define that a hydrogen bond between acetone and methanol molecule is formed when $r_{O-H_O} < 2.80$ Å. Similarly, the critical distance of the hydrogen bond between acetone and 1-propanol is chosen as 2.90 Å. The coordination numbers up to the first minimum calculated with the polarizable (fixed) charge model are 1.12 (1.09) and 1.01 (1.00) for methanol and 1-propanol, respectively.

We next calculated the probabilities of hydrogen bond formations between acetone and alcohol molecules. The probabilities of the number of hydrogen bonds, N_{HB}, are summarized in Table 2. In the fixed charge models, the probability of $N_{HB} = 1$ is the largest for both of the alcohols and the probabilities of $N_{HB} = 0$ and $N_{HB} = 2$ are similar. The probability of $N_{HB} \geq 3$ is quite small in both alcohols. Hence, the dynamics arising from $N_{HB} = 0$, 1, and 2 are considered in further discussion. By considering the polarization effect of solute, the probability of $N_{HB} = 1$ decreases and those of $N_{HB} = 0$ and 2 slightly increase. However, the probability of $N_{HB} = 1$ is

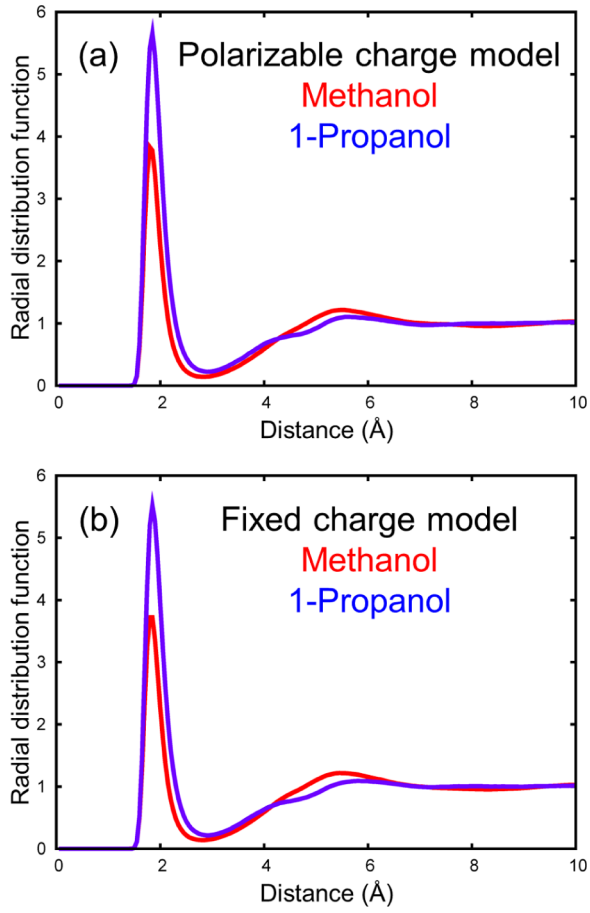

Figure 5. O(acetone)−H_O(alcohol) radial distribution function calculated with the (a) polarizable and (b) fixed charge models.

Table 2. Probabilities of the Number of Hydrogen Bonds Calculated from the MD Simulations

	polarizable charge model		fixed charge model	
N_{HB}	methanol	1-propanol	methanol	1-propanol
0	14.8%	18.1%	11.5%	15.0%
1	60.0%	64.2%	69.1%	71.4%
2	23.8%	17.0%	18.7%	13.3%
3	1.3%	0.8%	0.7%	0.3%
4	<0.1%	<0.1%	<0.1%	<0.1%

still more than 60% in both of the alcohols. These results are consistent with the experimental IR spectra (Figure 1a), though the contribution from $N_{HB} = 2$ is not distinguishable in the experimental IR spectra. It is conceivable, thus, that the IR peak arising from $N_{HB} = 2$ is hidden by the wide strong band arising from $N_{HB} = 1$ or the solute−solvent interaction is somewhat overestimated in the MD simulations.

To investigate the difference of the solute polarization by the number of hydrogen bonds, we calculated the averages and standard deviations of solute charges and dipole, and the distribution of dipole moment for $N_{HB} = 0$, 1, and 2 (Table 1 and Figure 6). Figure 6 clearly shows that the distribution of the total dipole moment is represented as the sum of three Gaussian distributions corresponding to $N_{HB} = 0$, 1, and 2. As the number of hydrogen bonds is increased, the average and standard deviation of solute dipole become large, which is caused by the polarization of the CO bond (Table 1). Although

dx.doi.org/10.1021/jp310621p | J. Phys. Chem. B 2013, 117, 4723−4731

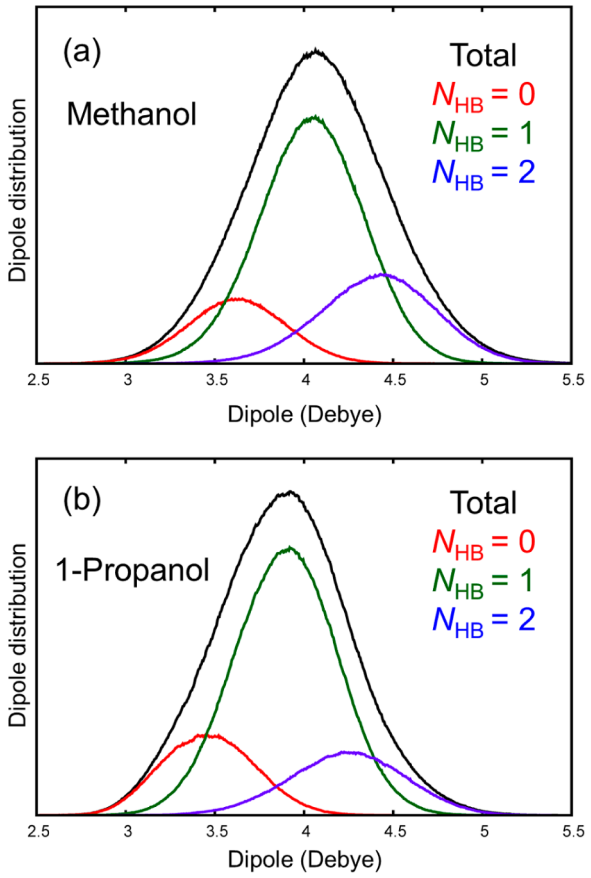

Figure 6. Distributions of dipole moment calculated from the MD simulations with the polarizable charge model: (a) methanol and (b) 1-propanol.

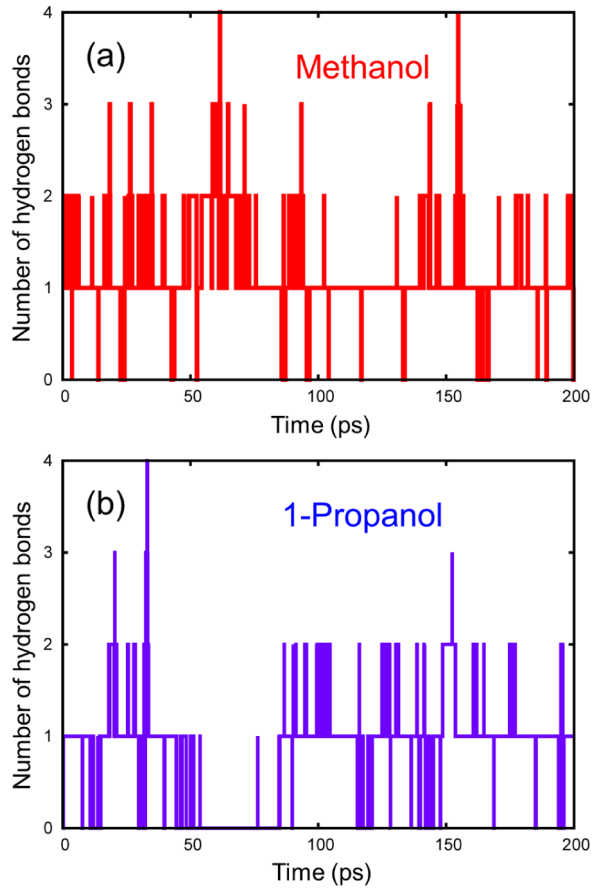

Figure 7. The number of hydrogen bonds in a 200 ps trajectory calculated with the polarizable charge model: (a) methanol and (b) 1-propanol.

the results of methanol and 1-propanol are similar to each other, the degree of polarization in 1-propanol is slightly smaller than that in methanol. Note that the averaged charges calculated without distinguishing the number of hydrogen bonds, which are used as the charges in the fixed charge model, are quite similar to the averaged charges for N_{HB} = 1. Thus, the solute−solvent interaction energy calculated with the polarizable charge model and N_{HB} = 2 is stronger than that with the fixed charge model, which results in the high probability of N_{HB} = 2 in the polarizable charge model (Table 3).

Table 3. Experimental and Calculated VER Times for the Acetone CO Stretching Mode

	experiment		polarizable charge model		fixed charge model	
N_{HB}	methanol	1-propanol	methanol	1-propanol	methanol	1-propanol
0	4.4	5.2	4.6	5.6	4.7	5.7
1	2.3	1.8	2.7	3.2	3.5	4.0
2			1.7	2.0	2.8	3.1

Figure 7 illustrates the time dependence of the number of N_{HB} in a 200 ps trajectory calculated with the polarizable charge model for both of the alcohols. N_{HB} changes from 0 to 4 in the range of a few ps to 10 ps. It is clear that the change of N_{HB} in methanol is much faster than that in 1-propanol. It is considered that slow hydrogen bond lifetimes of acetone in 1-propanol are due to the low number density of solvent molecules compared with those in methanol.

To examine the lifetime of a hydrogen bond more clearly, we calculated the hydrogen bond correlation function (HBCF), as shown in Figure 8. Here the HBCF was defined as

$$C(t) = \frac{\langle h(0)h(t)\rangle}{\langle h(0)h(0)\rangle} \quad (3)$$

where $h(t)$ = 1 if a specific hydrogen bond is created at time 0 and t and $h(t)$ = 0 otherwise. The HBCFs calculated with both of the charge models for both of the alcohols are well fitted by a biexponential function with two time scales of a few ps and 10−30 ps. Although, to the best of our knowledge, no experimental studies on the hydrogen-bond lifetime of acetone in alcohols have been reported, the hydrogen-bond lifetime of *N*-methylacetamide in methanol has been estimated to be 10−15 ps by time-resolved two-dimensional IR spectroscopy.[36]

We calculated the HBCFs only when N_{HB} = 1 at t = 0 (Figure S1, Supporting Information) and only when N_{HB} = 2 at t = 0 (Figure S2, Supporting Information). Figure S1 (Supporting Information) shows that the HBCFs sampled only when N_{HB} = 1 at t = 0 are well fitted by a single exponential function with the slow component of the fully sampled HBCFs shown in Figure 8. On the other hand, the HBCFs sampled only when N_{HB} = 2 at t = 0 (Figure S2, Supporting Information) are well fitted by a biexponential function with the two time constants of the fully sampled HBCFs, though the prefactors of the two components are

dx.doi.org/10.1021/jp310621p | J. Phys. Chem. B 2013, 117, 4723−4731

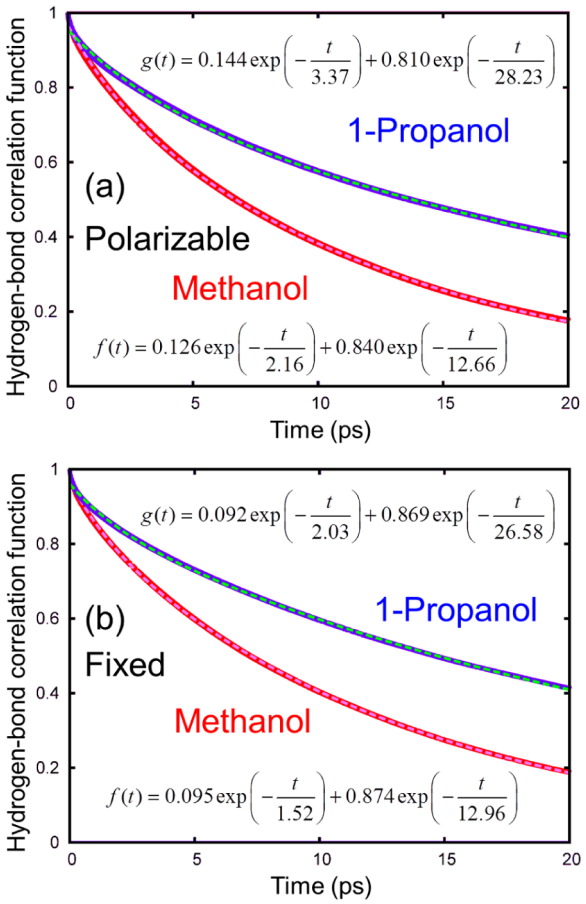

Figure 8. Hydrogen bond correlation functions calculated with the (a) polarizable and (b) fixed charge model.

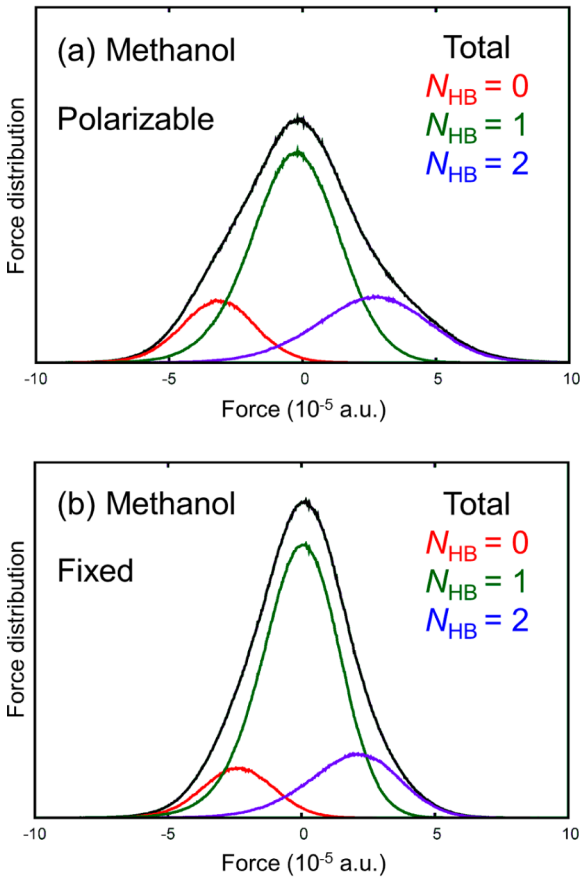

Figure 9. Distributions of force on the CO stretching mode of acetone in methanol calculated with the (a) polarizable and (b) fixed charge models.

different; that of the fast (slow) component is large (small) compared with those of the fully sampled HBCFs. The slow component in Figure S2 (Supporting Information) represents the dynamics which at least one hydrogen bond formed at $t = 0$ is broken during t. These results demonstrate that the fast component is mainly due to the contribution from $N_{HB} = 2$, while the slow component is due to the contribution from $N_{HB} = 1$.

Figure 8 shows that the polarization effect makes the fast component approximately 1.5 times slow, whereas that on the slow component is not significant. The result shows that the difference of the fast component between the polarizable and fixed charge models is due to the difference of the solute−solvent interaction energy in $N_{HB} = 2$.

We calculated the force, $F(t)$, on the solute CO stretching mode from the solvents. The CO stretching mode was determined by using the normal-mode analysis of acetone in the gas phase with M06-2X/6-311G(2d,2p) (Figure S3, Supporting Information). Figures 9 and S4 (Supporting Information) show the distributions of force, $\delta F = F - \langle F \rangle$ with $N_{HB} = 0$, 1, and 2. As the distribution of the dipole moment (Figure 5), the total distribution of the force is described as the sum of three Gaussian distributions corresponding to $N_{HB} = 0$, 1, and 2 and the force distributions are broad with the increase in N_{HB}. Furthermore, the comparison between two charge models shows that the polarization effect makes the distribution wide in both of the alcohols.

Figures 10 and S5 (Supporting Information) show the time-correlation function of force for each N_{HB}

$$\eta^{(k)}(t) = \langle \delta F(0)\delta F(t) \rangle_k \tag{4}$$

where the subscript k denotes N_{HB} at time $t = 0$. $\eta^{(k)}(0)$ represents the width of force distribution for $N_{HB} = k$; as noted above, $\eta^{(2)}(0) > \eta^{(1)}(0) > \eta^{(0)}(0)$. All $\eta^{(k)}(t)$ show there is a rapid oscillatory decay in the first hundreds of femtoseconds and a slow component with a time scale of picoseconds. We found that the oscillatory component is more prominent with the increase of N_{HB}. The slow component in 1-propanol is slower than that in methanol. The differences among $\eta^{(k)}(t)$ in the polarizable charge model are larger than those in the fixed charge model.

Figures 11 and S6 (Supporting Information) show the Fourier spectrum of the friction, $\hat{\eta}^{(k)}(\omega)$,

$$\hat{\eta}^{(k)}(\omega) = \int_0^\infty dt\, \cos(\omega t)\eta^{(k)}(t) \tag{5}$$

In both of the alcohols and both of the charge models, we found $\hat{\eta}^{(2)}(\omega) > \hat{\eta}^{(1)}(\omega) > \hat{\eta}^{(0)}(\omega)$ in a whole range of the frequencies. The peaks around 1400 cm^{-1} are due to the intramolecular vibrations of the alcohols, such as CO stretching and COH bending modes. Like $\eta^{(k)}(t)$, the differences among $\hat{\eta}^{(k)}(\omega)$ in the polarizable charge model are larger than those in the fixed charge model.

The VER time of the CO stretching mode of acetone, $T_1^{(k)}$, was evaluated from the Landau−Teller formula

dx.doi.org/10.1021/jp310621p | J. Phys. Chem. B 2013, 117, 4723−4731

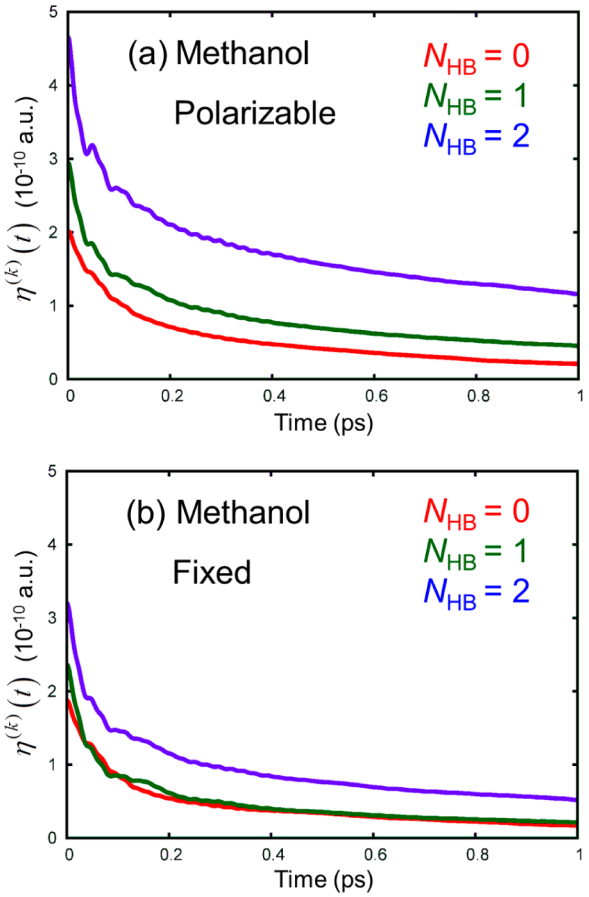

Figure 10. Force−force correlation functions in methanol calculated with the (a) polarizable and (b) fixed charge models.

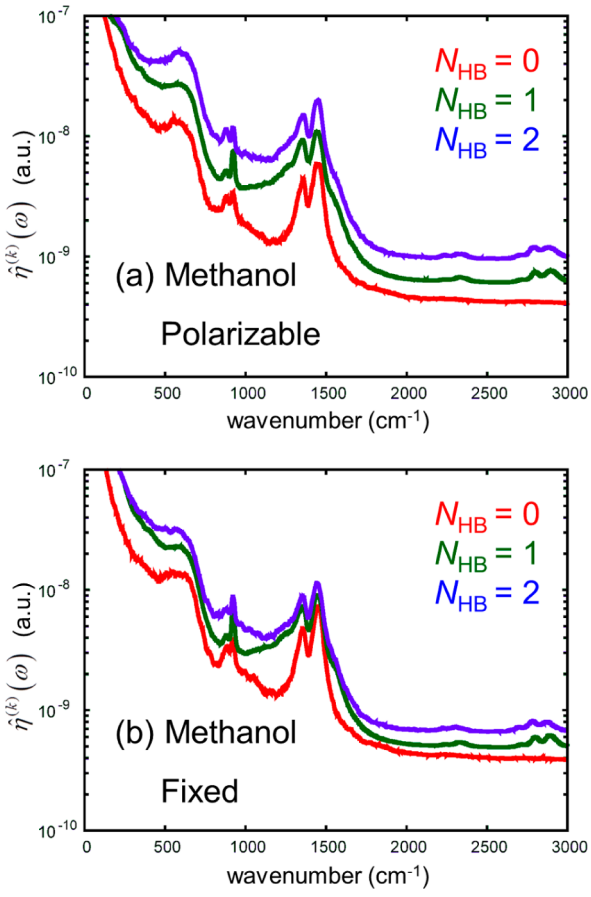

Figure 11. Fourier spectrum of force−force correlation functions in methanol calculated with the (a) polarizable and (b) fixed charge models.

$$\frac{1}{T_1^{(k)}} = f^{\mathrm{QM/CL}}(\omega_{\mathrm{CO}})\beta\hat{\eta}^{(k)}(\omega_{\mathrm{CO}}) \tag{6}$$

where $\beta = (k_B T)^{-1}$ with k_B being the Boltzmann constant and T the temperature, $f^{\mathrm{QM/CL}}$ is a quantum correction factor, and $\omega_{\mathrm{CO}} = 1700\ \mathrm{cm}^{-1}$, the frequency of the CO stretching mode. A quantum correction factor is required to satisfy the detailed balance condition, and various models have been proposed.[37−40] Since the main purpose of this study is to examine how the hydrogen bonds affect $T_1^{(k)}$, not to quantitatively calculate the values of $T_1^{(k)}$, we simply employed the harmonic model[39]

$$f^{\mathrm{QM/CL}}(\omega) = \frac{\beta\hbar\omega}{1 - \exp(-\beta\hbar\omega)} \tag{7}$$

where $\hbar$ is the Planck constant. Note that, for simplicity, we used the same frequency $\omega_{\mathrm{CO}} = 1700\ \mathrm{cm}^{-1}$ for all k (see also below).

The calculated VER times are summarized in Table 3 with experimental ones. The VER times calculated with the polarizable charge model for free acetone (N_{HB} = 0), 1:1 complex (N_{HB} = 1), and 1:2 complex (N_{HB} = 2) are 4.6, 2.7, and 1.7 ps in methanol and 5.6, 3.2, and 2.0 ps in 1-propanol, respectively. This result clearly shows the acceleration of the VER times by forming hydrogen bonds between acetone and solvent, about 60−80% acceleration per hydrogen bond. The VER times calculated with the fixed charge model are also given in Table 3. We found that the VER times for free acetone calculated with the fixed charge model are similar to those with the polarizable charge model in both alcohols. However, as the number of hydrogen bonds is increased, the difference between polarizable and fixed charge models becomes large: the VER times for 1:2 complex with the fixed charge model are 2.8 and 3.1 ps in methanol and 1-propanol, respectively, which are about 1.5 times slower than those with the polarizable charge model. Therefore, we found that the VER time of acetone with hydrogen bond(s) is largely affected by the solute polarization induced by solvent molecules. The effect of the solute polarization on the VER has been found in the VER of azide ion in water.[17]

To understand the origin of the difference by the number of hydrogen bonds and the difference between the polarizable and fixed charge models in detail, we decomposed δF into the sum of the force from the first solvation shell, i.e., from the solvent molecules directly forming hydrogen bonds with the solute, δF_{HB}, and the force from the others, $\delta F_{\mathrm{other}}$; $\delta F = \delta F_{\mathrm{HB}} + \delta F_{\mathrm{other}}$. Therefore, $\hat{\eta}^{(k)}(\omega)$ can be decomposed into the sum of three terms

$$\hat{\eta}^{(k)}(\omega) = \hat{\eta}^{(k)}_{\mathrm{HB}}(\omega) + \hat{\eta}^{(k)}_{\mathrm{other}}(\omega) + \hat{\eta}^{(k)}_{\mathrm{cross}}(\omega) \tag{8}$$

where

$$\hat{\eta}^{(k)}_{\mathrm{HB}}(\omega) = \int_0^\infty \mathrm{d}t\ \cos(\omega t)\langle\delta F_{\mathrm{HB}}(0)\delta F_{\mathrm{HB}}(t)\rangle_k \tag{9}$$

$$\hat{\eta}^{(k)}_{\mathrm{other}}(\omega) = \int_0^\infty \mathrm{d}t\ \cos(\omega t)\langle\delta F_{\mathrm{other}}(0)\delta F_{\mathrm{other}}(t)\rangle_k \tag{10}$$

dx.doi.org/10.1021/jp310621p | J. Phys. Chem. B 2013, 117, 4723−4731

Table 4. Decompositions of $\hat{\eta}^{(k)}(\omega)$ (in 10^{-10} au) at 1700 cm^{-1} with the Polarizable and Fixed Charge Models[a]

solvent	k	$\hat{\eta}^{(k)}(\omega)$	$\hat{\eta}^{(k)}_{HB}(\omega)$	$\hat{\eta}^{(k)}_{other}(\omega)$	$\hat{\eta}^{(k)}_{cross}(\omega)$
methanol	0	6.07 (6.03)	0.00 (0.00)	6.94 (6.85)	−0.86 (−0.82)
	1	10.45 (7.97)	4.72 (4.14)	6.57 (5.15)	−0.83 (−1.32)
	2	16.16 (9.92)	8.33 (5.58)	7.11 (5.95)	0.71 (−1.60)
1-propanol	0	5.01 (4.97)	0.00 (0.00)	5.95 (5.90)	−0.94 (−0.93)
	1	8.79 (7.03)	4.39 (3.83)	5.36 (4.39)	−0.96 (−1.19)
	2	13.87 (9.10)	7.15 (5.42)	6.15 (4.93)	0.57 (−1.26)

[a]Values in parentheses are for the fixed charge models.

and

$$\hat{\eta}^{(k)}_{cross}(\omega) = \int_0^\infty dt\, \cos(\omega t)(\langle \delta F_{HB}(0)\delta F_{other}(t)\rangle_k + \langle \delta F_{other}(0)\delta F_{HB}(t)\rangle_k) \quad (11)$$

Figures S7 and S8 (Supporting Information) illustrate $\hat{\eta}^{(k)}_{HB}(\omega)$ and $\hat{\eta}^{(k)}_{other}(\omega)$. (Since $\hat{\eta}^{(k)}_{cross}(\omega)$ is much smaller than $\hat{\eta}^{(k)}_{HB}(\omega)$ and $\hat{\eta}^{(k)}_{other}(\omega)$, $\hat{\eta}^{(k)}_{cross}(\omega)$ is not shown in the figures.) The shape of $\hat{\eta}^{(k)}_{HB}(\omega)$ is somewhat different from that of $\hat{\eta}^{(k)}_{other}(\omega)$; the peaks around 1400 cm^{-1} of $\hat{\eta}^{(k)}_{HB}(\omega)$ are much broader than those of $\hat{\eta}^{(k)}_{other}(\omega)$. The decompositions of $\hat{\eta}^{(k)}(\omega)$ at ω_{CO} are summarized in Table 4. The N_{HB} dependence of $\hat{\eta}^{(k)}(\omega)$ is mainly due to the force directly from hydrogen-bonding solvent, $\hat{\eta}^{(k)}_{HB}(\omega)$; the hydrogen bond accelerates the VER rate. It is interesting that, among the three terms, the differences of $\hat{\eta}^{(k)}_{other}(\omega)$ between the polarizable and fixed charge models are the largest when $k = 1$ and the smallest when $k = 2$. This is because the dipole moment of acetone with the polarizable charge model is larger than that with the fixed charge model when $N_{HB} = 2$. The difference with the polarizable charge model between methanol and 1-propanol is mainly due to $\hat{\eta}^{(k)}_{other}(\omega)$ when $k = 1$ and $\hat{\eta}^{(k)}_{HB}(\omega)$ and $\hat{\eta}^{(k)}_{other}(\omega)$ when $k = 2$, which results from the difference of number density of the OH polar group.

Although the present results qualitatively reproduce the acceleration of VER by the hydrogen bond, as seen in experimental results, the calculated accelerations are somewhat underestimated (even if the polarizable charge model is used). There are at least two possibilities for the underestimation. One is that we use the same ω_{CO} for the CO stretching mode. As written above, the frequency of the CO stretching mode decreases as N_{HB} increases: $\omega^{(0)}_{CO} > \omega^{(1)}_{CO} > \omega^{(2)}_{CO}$. Since $\hat{\eta}^{(k)}(\omega)$ monotonically decreases around 1700 cm^{-1} (Figures 11 and S6, Supporting Information), $T_1{}^{(k)}$ with $\omega^{(k)}_{CO}$ can be faster than $T^{(k)}_1$ with the fixed ω_{CO}. The other possibility is that the contribution of the 1:2 complex may contaminate the result of the 1:1 complex in the experimental result.

CONCLUSION

We studied the effect of a hydrogen bond on VER of the CO stretching mode of acetone in alcohol by sub-picosecond IR pump−probe spectroscopy and MD simulation. Similarly to the previous work on FL, the IR pump−probe experiment showed that VER of the hydrogen-bonded complex of acetone with alcohol is a few times faster than that of non-hydrogen-bonded acetone. In the MD simulation, we adopted the polarizable and fixed charge models for acetone to examine the effect of solute polarization. The VER rate of the CO stretching mode of acetone in alcohols was calculated with the Landau−Teller formula. The calculated results show that the VER rate is accelerated by the hydrogen bond between the acetone and solvent molecules. The acceleration is enhanced by the polarization of acetone due to the hydrogen bond interactions. The results calculated from the polarized model are in better agreement with the experimental ones than those from the fixed charged model. Therefore, the present result revealed that the solute polarization induced by solvent molecules plays important roles in the acceleration of the VER rate.

ASSOCIATED CONTENT

Supporting Information

Table of CRK matrix elements for acetone, detailed figures, and complete list of authors of refs 31 and 34. This material is available free of charge via the Internet at http://pubs.acs.org.

AUTHOR INFORMATION

Notes

The authors declare no competing financial interest.

ACKNOWLEDGMENTS

The computations were partly performed at the Research Center for Computational Science, Okazaki. This work was supported by the Joint Studies Program (2009-2012) of the Institute for Molecular Science, the Grant-in-Aid for JSPS Fellows (No. 23·238), Grant-in-Aid for Scientific Research (No. 22350013), and Grant-in-Aid for Challenging Exploratory Research (No. 23655020).

REFERENCES

(1) Desiraju, G. R.; Steiner, T. *The Weak Hydrogen Bond; In Structural Chemistry and Biology*; Oxford University Press: New York, 1999.
(2) Jeffrey, G. A. *An Introduction to Hydrogen Bond*; Oxford University Press: New York, 1997.
(3) Perrin, C. L.; Nielson, J. B. *Annu. Rev. Phys. Chem.* **1997**, *48*, 511−544.
(4) Nibbering, E. T. J.; Elsaesser, T. *Chem. Rev.* **2004**, *104*, 1887−1914.
(5) Fecko, C. J.; Loparo, J. J.; Roberts, S. T.; Tokmakoff, A. *J. Chem. Phys.* **2005**, *122*, 054506.
(6) Deak, J. C.; Rhea, S. T.; Iwaki, L. K.; Dlott, D. D. *J. Phys. Chem. A* **2000**, *104*, 4866−4875.
(7) Laenen, R.; Rauscher, C.; Laubereau, A. *Chem. Phys. Lett.* **1998**, *283*, 7−14.
(8) Cringus, D.; Yeremenko, S.; Pshenichnikov, M. S.; Wiersma, D. A. *J. Phys. Chem. B* **2004**, *108*, 10376−10387.
(9) Steinel, T.; Asbury, J. B.; Zheng, J. R.; Fayer, M. D. *J. Phys. Chem. A* **2004**, *108*, 10957−10964.
(10) Nienhuys, H. K.; Woutersen, S.; van Santen, R. A.; Bakker, H. J. *J. Chem. Phys.* **1999**, *111*, 1494−1500.
(11) Ohta, K.; Tominaga, K. *Chem. Phys.* **2007**, *341*, 310−319.
(12) Hong, X. Y.; Chen, S.; Dlott, D. D. *J. Phys. Chem.* **1995**, *99*, 9102−9109.
(13) Hirai, S.; Banno, M.; Ohta, K.; Palit, D. K.; Tominaga, K. *Chem. Phys. Lett.* **2007**, *450*, 44−48.

(14) Nitzan, A. *Chemical Dynamics in Condensed Phases*; Oxford University Press: New York, 2006.
(15) Bruehl, M.; Hynes, J. T. *Chem. Phys.* **1993**, *175*, 205−221.
(16) Chorny, I.; Vieceli, J.; Benjamin, I. *J. Chem. Phys.* **2002**, *116*, 8904−8911.
(17) Morita, A.; Kato, S. *J. Chem. Phys.* **1998**, *109*, 5511−5523.
(18) Staib, A. *J. Chem. Phys.* **1998**, *108*, 4554−4562.
(19) Fujisaki, H.; Yagi, K.; Straub, J. E.; Stock, G. *Int. J. Quantum Chem.* **2009**, *109*, 2047−2057.
(20) Skinner, J. L. *Theor. Chem. Acc.* **2011**, *128*, 147−155.
(21) Lawrence, C. P.; Skinner, J. L. *J. Chem. Phys.* **2002**, *117*, 5827−5838.
(22) Nguyen, P. H.; Stock, G. *J. Chem. Phys.* **2003**, *119*, 11350−11358.
(23) Lawrence, C. P.; Skinner, J. L. *J. Chem. Phys.* **2003**, *119*, 1623−1633.
(24) Li, S. Z.; Schmidt, J. R.; Skinner, J. L. *J. Chem. Phys.* **2006**, *125*, 244507.
(25) Park, S. M.; Nguyen, P. H.; Stock, G. *J. Chem. Phys.* **2009**, *131*, 184503.
(26) Bastida, A.; Soler, M. A.; Zuniga, J.; Requena, A.; Kalstein, A.; Fernandez-Alberti, S. *J. Phys. Chem. B* **2012**, *116*, 2969−2980.
(27) Jorgensen, W. L.; Maxwell, D. S.; Tirado-Rives, J. *J. Am. Chem. Soc.* **1996**, *118*, 11225−11236.
(28) Price, M. L. P.; Ostrovsky, D.; Jorgensen, W. L. *J. Comput. Chem.* **2001**, *22*, 1340−1352.
(29) Ponder, J. *TINKER*, version 3.5; Washington University: St. Louis, MO, 1997.
(30) Higashi, M.; Truhlar, D. G. *AMBERPLUS*, version 2010; University of Minnesota: Minneapolis, MN, 2010.
(31) Case, D. A.; Darden, T. A.; Cheatham, T. E., III; Simmerling, C. L.; Wang, J.; Duke, R. E.; Luo, R.; Walker, R. C.; Zhang, W.; Merz, K. M.; et al. *AMBER*, version 11; University of California: San Francisco, CA, 2010.
(32) Morita, A.; Kato, S. *J. Am. Chem. Soc.* **1997**, *119*, 4021−4032.
(33) Zhao, Y.; Truhlar, D. G. *Theor. Chem. Acc.* **2008**, *120*, 215−241.
(34) Schmidt, M. W.; Baldridge, K. K.; Boatz, J. A.; Elbert, S. T.; Gordon, M. S.; Jensen, J. H.; Koseki, S.; Matsunaga, N.; Nguyen, K. A.; Su, S. J.; et al. *J. Comput. Chem.* **1993**, *14*, 1347−1363.
(35) Dorosh, O.; Kisiel, Z. *Acta Phys. Pol., A* **2007**, *112*, S95−S104.
(36) Woutersen, S.; Mu, Y.; Stock, G.; Hamm, P. *Chem. Phys.* **2001**, *266*, 137−147.
(37) Schofield, P. *Phys. Rev. Lett.* **1960**, *4*, 239−240.
(38) Oxtoby, D. W. *Adv. Chem. Phys.* **1981**, *47*, 487−519.
(39) Bader, J. S.; Berne, B. J. *J. Chem. Phys.* **1994**, *100*, 8359−8366.
(40) Skinner, J. L.; Park, K. *J. Phys. Chem. B* **2001**, *105*, 6716−6721.